

HILLOCK DEFECTS IN InGaAs/InP MULTI-LAYERS GROWN BY MBE

Hideho SAITO, John O. BORLAND *, Hajime ASAH, Haruo NAGAI and Kiyoshi NAWATA

Atsugi Electrical Communication Laboratory, Nippon Telegraph and Telephone Public Corporation, Atsugi-shi, Kanagawa 243-01, Japan

Received 6 June 1983; manuscript received in final form 15 September 1983

Common macroscopic defects on (001) InGaAs/InP multi-layers grown by molecular beam epitaxy (MBE) are hillock defects elongated along the $\langle 1\bar{1}0 \rangle$ orientation. The morphology of these hillock defects has been investigated by selective chemical etching and transmission electron microscopy (TEM). The hillock defects were classified into: (i) smaller hillocks with no noticeable structural defects and (ii) larger hillocks with stacking faults and dislocations. It is also shown that the phosphorus source condition and the substrate surface cleaning condition play an important role in the formation of larger hillocks and smaller hillocks, respectively.

1. Introduction

Semiconductor lasers with InGaAsP/InP and InGaAs/InP multi-layer structures have been studied extensively as light sources for optical communication systems in the 1.0–1.7 μm wavelength region. The relationship between device performance and crystal defects was well investigated for laser crystals grown by liquid phase epitaxy (LPE) [1]. Recently, room temperature CW operation of MBE (molecular beam epitaxy) grown InGaAs/InP DH laser crystals was reported [2]. However, crystal defects in InGaAs/InP multi-layers grown by MBE have not been sufficiently investigated and evaluated. Hillocks, called “oval defect”, in GaAs layers grown by MBE are well known and the morphology of the hillocks has been well investigated and reported [3–6].

Similar defects were observed in MBE grown InGaAs/InP multi-layers. This report describes the morphology of the hillock defects and presents the results of a study on defect characterization by selective chemical etching, Nomarski contrast microscopy, scanning electron microscopy (SEM), transmission electron microscopy (TEM) and Auger electron spectroscopy (AES).

* Department of Material Science and Engineering, Massachusetts Institute of Technology, Cambridge, Massachusetts 02139, USA.

2. Experimental

The MBE system used here is the same as that described elsewhere [7,8]. The system has an airlock mechanism so that the substrate can be set onto a substrate holder without breaking the vacuum in the growth chamber. The effusion cells are mounted at the bottom of the growth chamber with a vertical configuration. In this experiment, In–Ga alloy and In, contained in pyrolytic BN crucible cells, were used as group III beam sources. Red phosphorus and arsenic were used as group V beam sources (P_4 and As_4).

The substrates used here were Sn-doped ($n =$

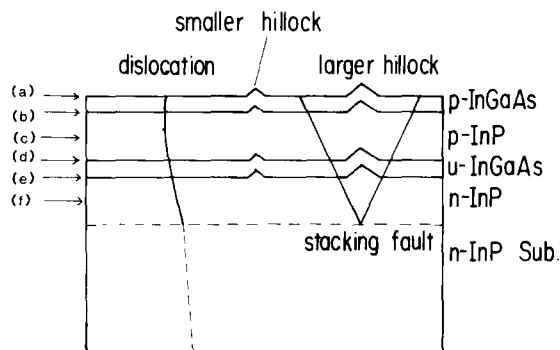


Fig. 1. MBE-grown InGaAs/InP multi-layer structure and schematic configuration of the defects under study (not to scale); (a)–(f) correspond to figs. 6a–6f, respectively.

$(1-2) \times 10^{18} \text{ cm}^{-3}$) and Fe-doped semi-insulating (001) InP. The etch pit density for these substrates was about $3 \times 10^5 \text{ cm}^{-2}$. After Br-methanol chemical etching, the substrates were mounted on the Mo block by using In solder. Just prior to growth of the first InP layer, a flash heat treatment at 480°C for 1 min under a phosphorus vapor pressure (2.4×10^{-6} Torr) was carried out on the InP substrate except when the effect of the substrate surface treatment process on the hillock density was studied.

InP layers were grown at a substrate temperature of approximately 450°C and at a growth rate of $1 \mu\text{m/h}$. InGaAs layers were grown at a substrate temperature of about 480°C and a $1 \mu\text{m/h}$ growth rate. The MBE-grown InGaAs/InP multi-layer structure wafers used for this experiment are composed of (i) an Sn-doped n-type InP cladding layer (first layer), (ii) an undoped InGaAs active layer (second layer), (iii) an Mn- or Be-doped p-type InP cladding layer (third layer) and (iv) an Mn- or Be-doped p-type InGaAs layer (fourth layer), as shown in fig. 1.

Selective chemical etching was carried out in order to investigate the hillock propagation between layers, and the relationship between hillocks and crystal defects. Selective etchants used were sulfuric acid solution, composed of 3 vol. H_2SO_4 : 1 vol. H_2O_2 : 1 vol. H_2O for InGaAs, which attacks InGaAs but does not attack InP, and hydrobromic acid solution, composed of 1 vol. HBr : 2 vol. H_3PO_4 for InP, which is known as a defect etching solution for InP [9] and does not attack InGaAs.

The TEM samples were prepared in the following manner to observe the defects in the region near the surface of the p-InP cladding layer (third layer). The p-InGaAs cap layer (fourth layer) was removed by sulfuric acid solution. The surface of the p-InP layer (third layer) was protected by using wax, and the chemical etching was performed to remove the n-InP substrate and n-InP cladding layer (first layer) by 10 vol. HBr : 1 vol. HF solution, and undoped InGaAs active layer (second layer) by sulfuric acid solution. Then, the samples were mounted on meshes and were thinned to foils of $\sim 0.5 \mu\text{m}$ thick by ion milling. The foils were observed with a transmission electron microscope (JEOL-200B) at 200 kV electron energy.

3. Results and discussion

The surface morphology of MBE-grown InGaAs/InP multi-layers was studied, first of all, using Nomarski contrast microscopy and scanning electron microscopy (SEM). Hillocks similar to those observed in MBE-grown GaAs were observed, as shown in fig. 2. The hillock size ranged from 2 to $15 \mu\text{m}$ and the height ranged from 300 to 3000 Å. These hillock defects can be classified into: smaller hillocks (height ~ 300 Å) and larger hillocks (height ~ 1500 Å). The smaller hillocks have a willow leaf (elongated oval defect) shape structure, indicated by A in fig. 2. Their long axes were aligned along the $\langle 1\bar{1}0 \rangle$ orientation. The larger hillocks have an ellipse shape structure. They were also elongated along the $\langle 1\bar{1}0 \rangle$ direction, indicated by B in fig. 2. Most of the larger hillocks appear to have a nucleus at their center. The density of the smaller hillocks was about 10^5 cm^{-2} , while the density of the larger hillocks was about 10^3 cm^{-2} . The overgrowth delineates a regular edge on the top of the smaller hillocks, as shown in the SEM photographs of fig. 3a. For the larger hillocks, this edge blurs as shown in fig. 3b.

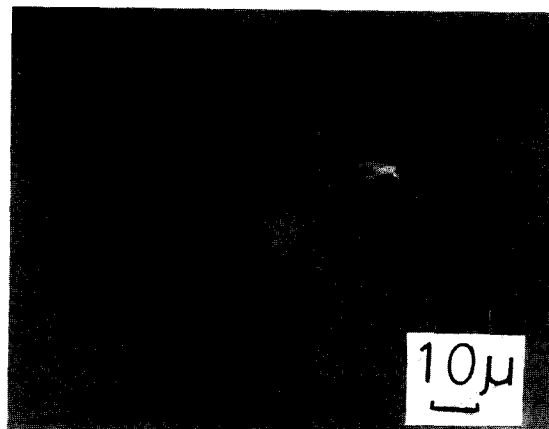


Fig. 2. Nomarski contrast micrograph of as-grown surface of InGaAs/InP multi-layers grown by MBE. Smaller hillock (height 300 Å) is indicated by A. Larger hillock (height 1500 Å) is indicated by B.

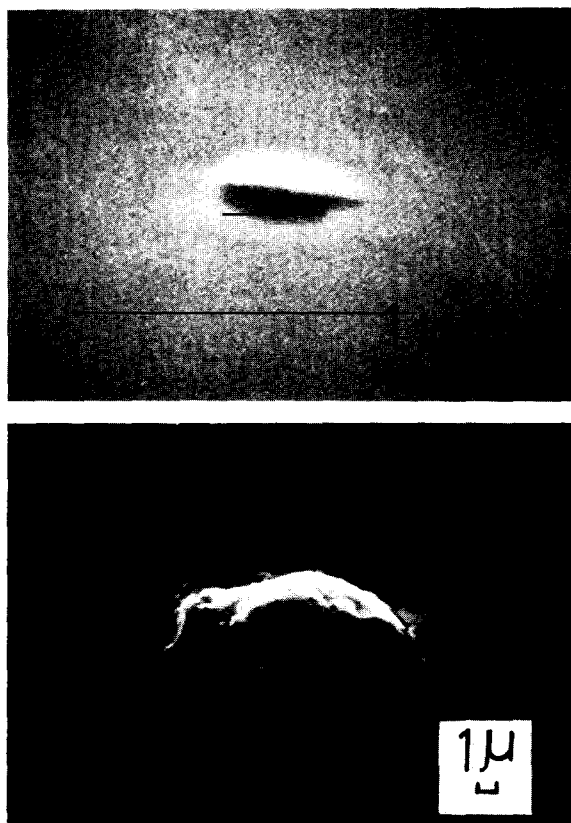


Fig. 3. SEM micrographs of the hillocks: (a) smaller hillock; (b) larger hillock.

3.1. Larger hillocks

To investigate the nature of the larger hillocks, TEM observations were carried out. Fig. 4 shows TEM photographs in the region near the surface of the p-InP cladding layer (third layer). It is clear that stacking faults and dislocations exist in the larger hillock. The contrast of the trapezoid elongated along the $\langle 110 \rangle$ direction disappears for (220) reflection (fig. 4a), and the contrast of the trapezoid elongated along the $\langle \bar{1}\bar{1}0 \rangle$ direction disappears for (2 $\bar{2}$ 0) reflection (fig. 4b). No extra spots are observed in the selected area electron diffraction patterns of these trapezoids. These results mean that these trapezoids are stacking faults. From a consideration of the length of the cross section between faults and a sample foil, the stacking faults in fig. 4 originate from near the interface between the n-type substrate and the n-type InP

cladding layer (first layer), as shown in fig. 1. The character of these faults cannot be decided on, because two faults pile up.

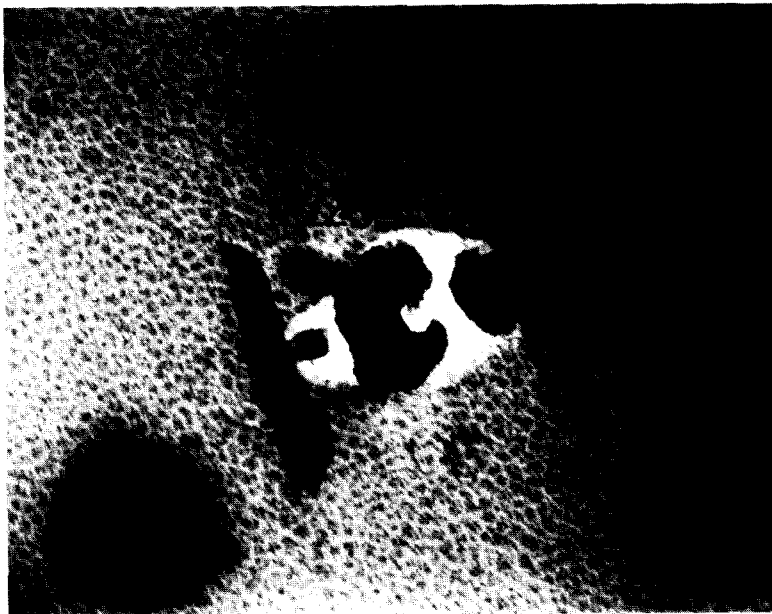
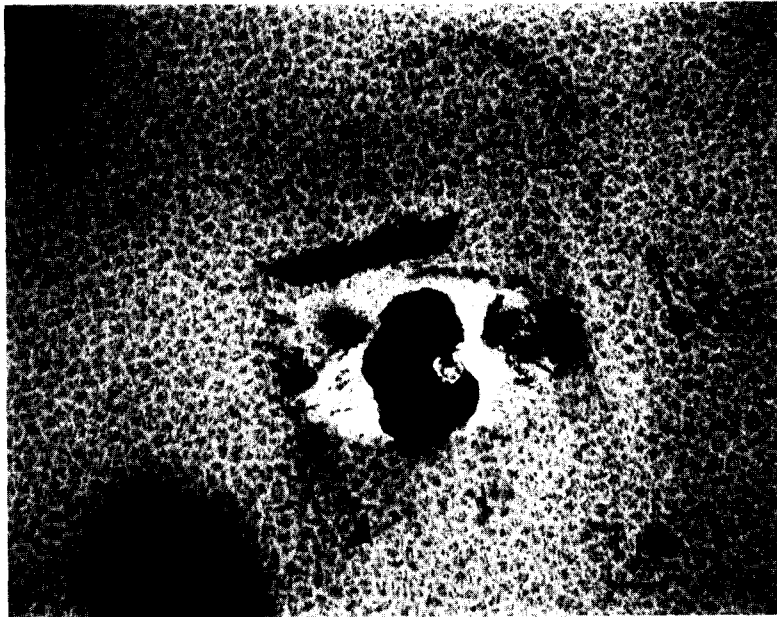
High density dislocations also exist around the larger hillocks. Moreover, dark contrast defects exist in the center of the larger hillocks, as also shown in fig. 4a and 4b. The electron diffraction patterns selected from the central region of the larger hillocks are shown in fig. 4c. The diffraction patterns are composed of diffraction spots and rings. These patterns reveal the polycrystalline nature of InP as well as the single crystal nature of InP. Electron beams cannot be transmitted through the dark contrast defects. Therefore, these results indicate that InP polycrystals have grown around the dark contrast defects.

The central region of the larger hillocks was also studied by Auger electron spectroscopy. Auger measurements were carried out on the slightly Ar ion etched surfaces. The results of the Auger measurements are shown in table 1, where the Auger signal ratios of In/P and O/P are listed. The ratios from the flat region (InP single crystal region) are also shown. In the central region of the larger hillocks, In/P and O/P are increased, compared with those from the flat region. This indicates that more indium is contained in the central region (probably in dark contrast defects), although the detected oxygen signal is considered to come from adsorbed oxygen atoms on the wafer surface.

It has been observed that the phosphorus source condition plays an important role in the formation of larger hillocks. When a phosphorus source (red phosphorus) stored in a dessicator was used, the density of the larger hillocks was about 10^4 cm^{-2} . The density increased when growth was repeated. For this case, a considerable amount of white powder was observed in the phosphorus crucible cell when the growth chamber was opened to recharge the phosphorus source. On the other hand, the use of a phosphorus source stored in an evacuated ampoule reduced the amount of white powder and the density of the larger hillocks by one or two orders of magnitude. Red phosphorus easily absorbs water and easily oxidizes. Therefore, this white powder seems to be phosphorus oxide. Perhaps, this white powder (phosphorus oxide particles) adheres accidentally to the wafer surface

during growth. These adsorbed phosphorus oxides will decompose and form indium oxides on the wafer surface by combining with impinging indium. The overgrowth occurs around these indium oxides and the InP polycrystals are formed in the

central region of the larger hillocks. Although the formation mechanism of the larger hillocks must be studied in more detail, it is very important to shut out the air from the phosphorus source, in order to eliminate larger hillocks.



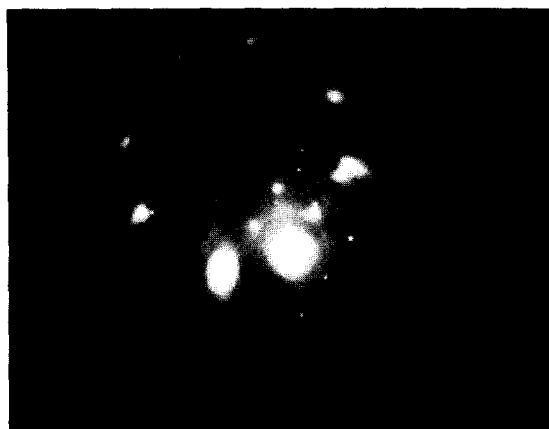


Fig. 4. TEM micrographs of the region around the larger hillock: (a) (220) reflection; (b) $(\bar{2}\bar{2}0)$ reflection; (c) electron diffraction pattern selected from the central region of the larger hillock.

3.2. Smaller hillocks

In contrast to the larger hillocks, near the smaller hillocks there are no noticeable structural defects, such as dislocations or stacking faults, as shown in the TEM photograph (fig. 5). Moreover, no extra spots or diffraction rings were observed in the diffraction patterns. The monocrystalline nature of this region was revealed.

In order to investigate the propagation of smaller hillocks between layers grown by MBE, selective etchants were used. The etching process showed that the hillocks propagated from the lower layer to the upper layer. The Nomarski contrast micrographs, figs. 6a–6f, correspond to the etching steps indicated by (a)–(f), respectively, in fig. 1. The wafer shown in fig. 6 is composed of (i) an n-type InP cladding layer (first layer, $0.8 \mu\text{m}$), (ii)

an undoped InGaAs active layer (second layer, $0.2 \mu\text{m}$), (iii) a p-type InP cladding layer (third layer, $1.6 \mu\text{m}$) and (iv) a p-type InGaAs cap layer (fourth layer, $0.3 \mu\text{m}$).

Fig. 6a shows the as-grown surface of the p-InGaAs layer (fourth layer), in which two smaller hillocks exist. Fig. 6b shows the surface of the p-InP layer (third layer), in which two smaller hillocks exist, after removal of the p-InGaAs cap layer (fourth layer, $0.3 \mu\text{m}$) by sulfuric acid solution. These hillocks correspond exactly to those in fig. 6a.

Fig. 6c shows the p-InP (third layer) surface after etching the p-InP cladding layer (third layer) by hydrobromic acid solution, in which hillocks are blurred by the etching process and some etch pits appear. These etch pits correspond to dislocations [9]. It is noteworthy that the smaller hillocks observed in fig. 6c do not correspond to these etch pits. This indicates that the smaller hillocks do not relate to dislocations, as can also be seen in fig. 5.

Fig. 6d shows the surface of the undoped InGaAs active layer (second layer), in which two hillocks exist, after removal of the p-InP cladding layer (third layer, $1.6 \mu\text{m}$) by hydrobromic acid solution. These hillocks correspond exactly to those in figs. 6a and 6b. Fig. 6e shows the surface of the n-InP cladding layer (first layer), in which two smaller hillocks exist, after removal of the InGaAs

Table 1
Results of Auger measurements on the InP layer surface

	Auger intensity ratio	
	In/P	O/P
Central regions of larger hillocks	11.7	2
	11	2.3
Flat regions (InP single crystal)	6.1	0.8
	5.8	0.75
	5.7	0.9

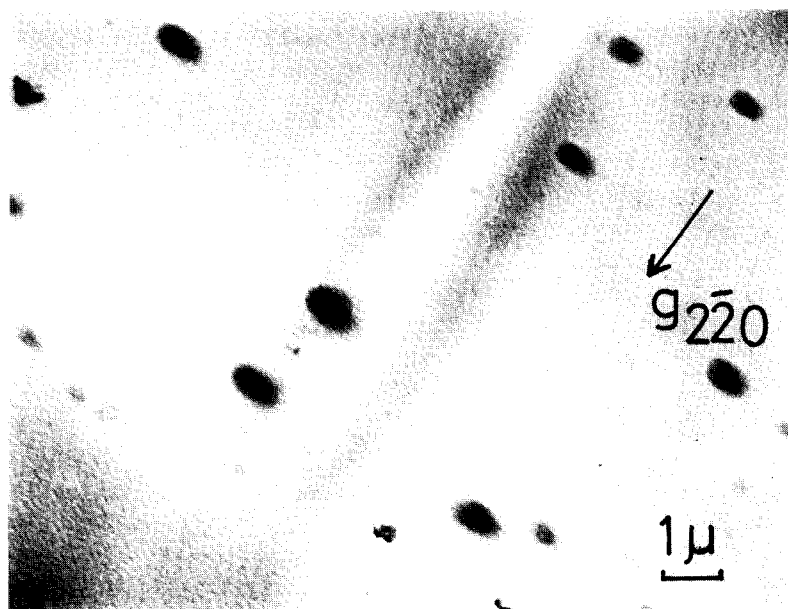


Fig. 5. TEM micrograph of the region around the smaller hillock.

active layer (second layer, $0.2 \mu\text{m}$) by sulfuric acid solution. These hillocks correspond to those in figs. 6a, 6b and 6d. This result means that hillocks propagate from the lower layer to the upper layer. Other than this propagation, the size and the height of these hillocks hardly change.

Fig. 6f shows the surface of the n-InP cladding layer (first layer), in which some etch pits appear, after etching of the n-InP by hydrobromic acid solution. These etch pits also correspond to the etch pits shown in fig. 6c. This means that etch pit defects propagate from the lower layer to the upper layer.

From the above observation, it is clear that smaller hillocks propagate from the lower layer to the upper layer, as shown in fig. 1. Etch pit defects also propagate from the lower layer to the upper layer [10]. However, these smaller hillocks do not relate to etch pit defects (dislocations). It is odd that smaller hillocks involve no structural defects, such as dislocations or stacking faults, but propagate from the lower layer to the upper layer.

The substrate surface treatment (thermal cleaning) process effect – before growth – on the den-

sity of the smaller hillocks was studied, where the same chemical preparation process as that described above was carried out for the substrates. First of all, the phosphorus vapor pressure during the cleaning process at 480°C was changed from 2.4×10^{-6} to 1×10^{-6} Torr. The density of the smaller hillocks did not depend on the phosphorus vapor pressure. However, the thermal cleaning of the substrate under phosphorus vapor pressure (2.4×10^{-6} Torr) at 450°C for 1 min caused an increase in the density of the smaller hillocks (10^6 cm^{-2}), as shown in fig. 7a. This is probably because the degree of removing of substrate surface contamination is poor. On the other hand, thermal cleaning of the substrate under arsenic and phosphorus ($\approx 1:3$) vapor pressure (total pressure is about 2.4×10^{-6} Torr) at 520°C for 4 min improved the degree of removing of substrate surface contamination and reduced the smaller hillock density by about one order of magnitude (10^4 cm^{-2}), as shown in fig. 7b. These results indicate that the substrate surface thermal cleaning condition plays an important role in the formation of smaller hillocks.

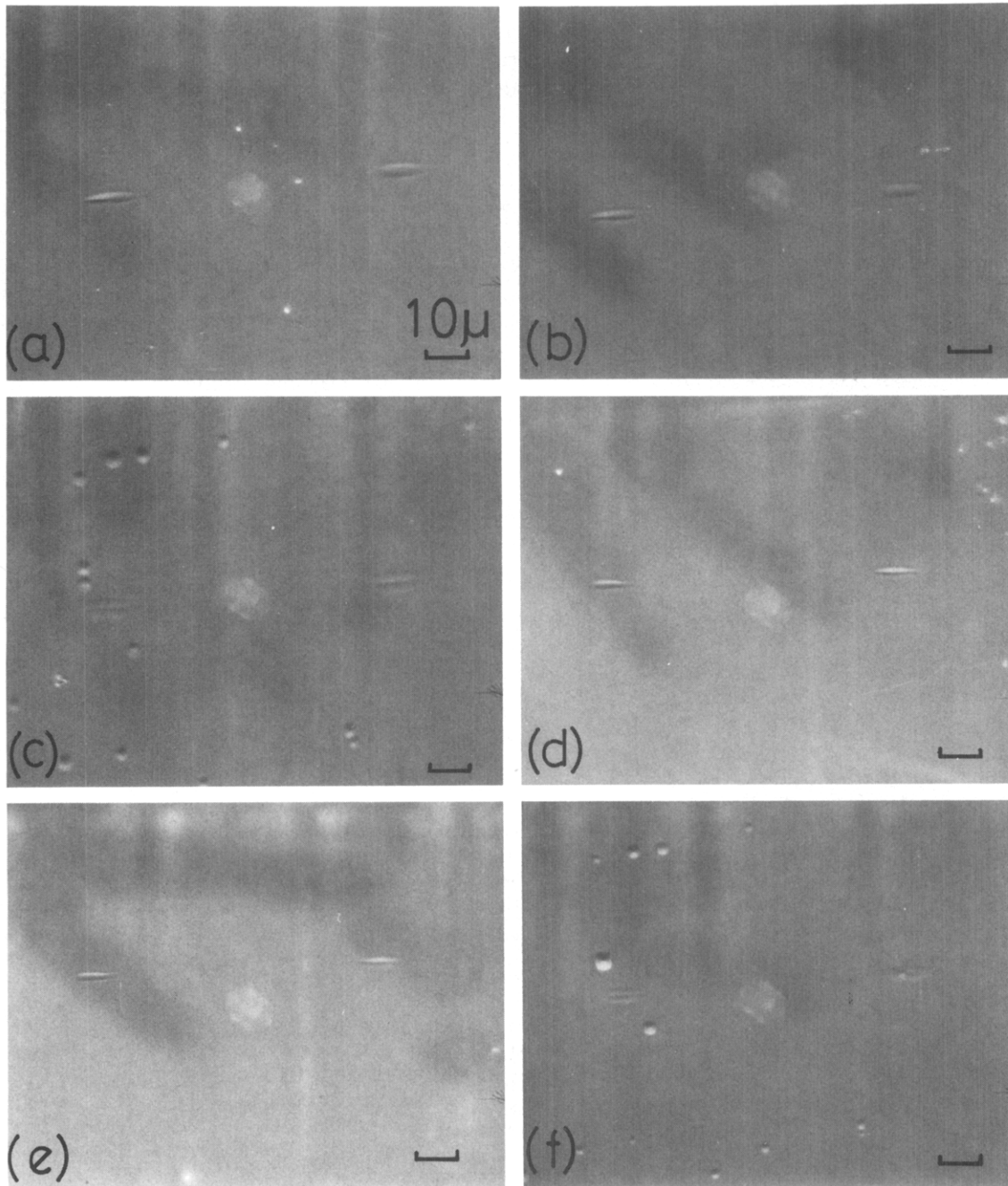


Fig. 6. Nomarski contrast micrographs: (a) as grown surface on the cap p-InGaAs layer (fourth layer); (b) p-InP clad layer (third layer) surface; (c) p-InP clad layer (third layer) surface after p-InP layer defect etching; (d) undoped InGaAs active layer (second layer) surface; (e) n-InP clad layer (first layer) surface; (f) n-InP clad layer (first layer) surface after n-InP layer defect etching.

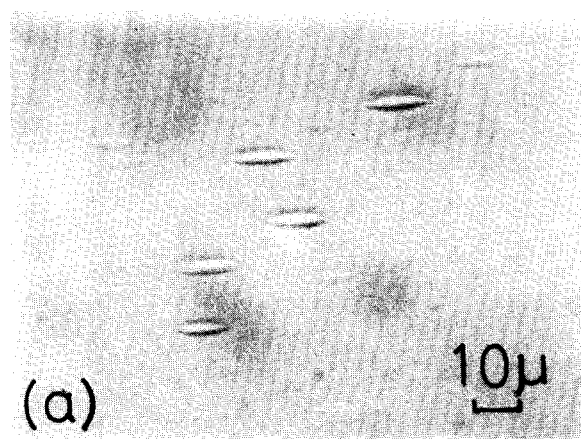


Fig. 7. Dependence of smaller hillock density on substrate surface treatment before growth: (a) thermal cleaning of substrate surface under phosphorus vapor pressure at 450°C for 1 min; (b) thermal cleaning of substrate surface under arsenic and phosphorus vapor pressure at 520°C for 4 min.

4. Summary

On (001) InGaAs/InP multi-layers grown by MBE, hillock defects, elongated along the $\langle 110 \rangle$

- (i) There were no noticeable structural defects associated with the smaller hillocks (height 300 Å).
- (ii) There were stacking faults and high density dislocations associated with the larger hillocks (height 1500 Å).

These results make it possible to establish the tentative configuration shown in fig. 1 for these hillocks.

It was also shown that the phosphorus source condition plays an important role in the formation of larger hillocks. In order to eliminate the larger hillocks, it was very important to shut out the air from the phosphorus source. Moreover, the substrate thermal cleaning condition was an important factor in the formation of smaller hillocks.

Acknowledgements

The authors wish to thank M. Fujimoto, T. Ikegami and K. Kurumada for their encouragement throughout the work.

References

- [1] T. Kotani, S. Komiya, S. Nakai and Y. Yamaoka, *J. Electrochem. Soc.* 127 (1980) 2273.
- [2] Y. Kawamura, Y. Noguchi, H. Asahi and H. Nagai, *Electron. Letters* 18 (1982) 91.
- [3] C.E.C. Wood, L. Rathbun, H. Ohno and D. Desimone, *J. Crystal Growth* 51 (1981) 299.
- [4] R.Z. Rachtach and B.S. Krusor, *J. Vacuum Sci. Technol.* 18 (1981) 756.
- [5] Y.G. Chai and R. Chow, *Appl. Phys. Letters* 38 (1981) 796.
- [6] M. Bafleur, A. Munoz-Yague and A. Roehen, *J. Crystal Growth* 59 (1982) 531.
- [7] H. Asahi, Y. Kawamura, M. Ikeda and H. Okamoto, *J. Appl. Phys.* 52 (1981) 2852.
- [8] Y. Kawamura, H. Asahi, M. Ikeda and H. Okamoto, *J. Appl. Phys.* 52 (1981) 3445.